Fingerpick Blood-Based Nucleic Acid Testing on A USB Interfaced Device Towards HIV Self-Testing

Tianyi Liu[1], Gihoon Choi[1], Zifan Tang[1], Aneesh Kshirsagar[1], Anthony J Politza[2], and Weihua Guan[1, 2]*

[1] Department of Electrical Engineering, Pennsylvania State University, University Park, Pennsylvania 16802, United States

[2] Department of Biomedical Engineering, Pennsylvania State University, University Park, Pennsylvania 16802, United States

* Corresponding Author, Email: w.guan@psu.edu, Tel: 1-814-867-5748

Abstract

HIV self-testing is an emerging innovative approach that allows individuals who want to know their HIV status to collect their own specimen, perform a test, and interpret the results privately. Existing HIV self-testing methods rely on rapid diagnostic tests (RDTs) to detect the presence of HIV-1/2 antibodies, which could miss a significant portion of asymptomatic carriers during the window period. In this work, we present a fully integrated nucleic acid testing (NAT) device towards streamlined HIV self-testing using 100 μL finger-prick whole blood. The device consists of a ready-to-use microfluidic reagent cartridge and an ultra-compact NAT-on-USB analyzer. The test requires simple steps from the user to drop the finger-prick blood sample into a collection tube with lysis buffer and load the lysate onto the microfluidic cartridge, and the testing result can be easily read out by a custom-built graphical user interface (GUI). The microfluidic cartridge and the analyzer automatically handle the complexity of sample preparation, purification, and real-time reverse-transcription loop-mediated isothermal amplification (RT-LAMP). With a turnaround time of ~60 min, we achieved a limit of detection (LoD) of 214 viral RNA copies/mL of whole blood at a 95% confidence level. Due to its ease of use and high sensitivity, we anticipate the HIV NAT-on-USB device would be particularly useful for the high-risk populations seeking private self-testing at the early stages of exposure.

Keywords: HIV, Self-Testing, Point-of-care Testing, RT-LAMP, Nucleic Acid Testing

1 Introduction

According to the World Health Organization (WHO), HIV continues to be a significant global public health issue, having claimed 36.3 million lives so far (WHO 2021). Early and accurate HIV diagnosis is a critical step to initiate timely antiretroviral therapy (ART), which could suppress HIV, stop the progression of HIV disease, and reduce the viral load (VL) to undetectable levels (Zolopa 2010). The Joint United Nations Program on HIV/AIDS (UNAIDS) has thus put forth the ambitious goal to end AIDS as a global public health threat by 2030. This goal will highly depend on the increases in HIV testing, treatment, and viral suppression to prevent the onward transmission of HIV (Iwuji and Newell 2017). To this end, HIV self-testing is proposed as a new approach where an individual who wants to know HIV status collects a specimen, performs a test, and interprets the result privately (Parekh et al. 2018; Spielberg et al. 2004). In recent years, uptake of HIV self-testing has gained increasing acceptance both in the US and internationally (Frith 2007; Frye and Koblin 2017; Johnson and Corbett 2016; Ng and Tan 2013; Spielberg et al. 2004).

Existing HIV self-testing methods rely exclusively on widely adopted RDTs to detect the presence of HIV-1/2 antibodies(Fund 2022). While HIV RDT is very well suited for the primary screening process due to its low cost and fast turnaround time (de la Fuente et al. 2012; Mugo et al. 2017; Ng et al. 2012; Sarkar et al. 2016), it could miss a significant portion of asymptomatic HIV carriers during the 2-4 weeks of the window period (Parekh et al. 2018; Stone et al. 2018). A possible alternative is to use nucleic acid testing (NAT), one of the most sensitive methods available for identifying the presence of HIV RNA and/or DNA (Parekh et al. 2018). NAT devices for HIV testing are readily available in centralized labs. However, a NAT device suitable for HIV self-testing is still lacking. In a recent report (Mazzola and Pérez-Casas 2015), WHO surveyed a list of HIV detection platforms such as Aptima HIV-1 Quant Assay (Hologic), GeneXpert HIV-1 Viral Load Test (Cepheid), Alere q system (Alere), cobas LiatTM System (Roche), and EOSCAPE-HIVTM HIV Rapid RNA Assay system (Wave 80 Biosciences). Most of these systems rely on relatively complex and expensive analyzers and replace conventional real-time PCR machines with portable thermal cyclers (Mauk et al. 2017). They often require plasma as a testing specimen which is prepared from venipuncture whole blood in laboratory conditions. Thus these NAT devices are not well suited for self-testing, in which a self-obtainable sample type such as finger-prick whole blood (Bertagnolio et al. 2010; Fidler et al. 2017; Guichet et al. 2018) or oral fluid would be preferred. To make the technologically intense HIV NATs more readily available

in the resource-limited setting such as self-testing, there are increasing efforts in developing alternative isothermal amplification techniques that do not require thermal cycling and expensive instrumentation (Choi et al. 2018; Choi et al. 2016; Curtis et al. 2016; Curtis et al. 2012; Damhorst et al. 2015; Liu et al. 2011; Mauk et al. 2017; Myers et al. 2013; Phillips et al. 2018; Safavieh et al. 2016; Singleton et al. 2014). These assays include loop-mediated isothermal amplification (LAMP), nucleic acid sequence-based amplification (NASBA), recombinase polymerase amplification (RPA), as well as helicase-dependent amplification (HDA). Among isothermal methods, LAMP has been observed to be more resistant than PCR to inhibitors in complex samples such as blood (Wang et al. 2014). HIV LAMP assay (Curtis et al. 2014; Curtis et al. 2008, 2009; Ocwieja et al. 2015; Odari et al. 2015; Rudolph et al. 2015) has enabled the recent development of point-of-care HIV NAT devices, such as Smart Cup (Liao et al. 2016) and microRAAD (Phillips et al. 2019). Despite significant progress, no HIV NAT technologies can be used by a layperson to perform self-testing due to the complexity in sample handling (Dineva et al. 2007).

An ideal HIV self-test should combine the benefits of RDTs (minimal training, minimal sample handling, and rapid) and NAT (highly sensitive, specific, and quantitative capability). To this end, it would require a fully integrated sample preparation by automating the assay process with a cost-effective microfluidic chip and analyzer. Here, we present an integrated 'finger-prick blood sample in, answer out' HIV NAT device to address this challenge. The device consists of a microfluidic reagent cartridge and an ultra-compact NAT-on-USB analyzer. We showed that the device can work with a reduced whole blood volume of 100 µL (readily available with finger-pick method) as compared to traditional methods using ~10 ml of venous blood(LabCorp). The test requires simple steps from the user to drop the finger-prick blood sample into a collection tube with lysis buffer and load the lysate onto the microfluidic cartridge, and the testing result can be easily read out on a custom-built graphical user interface (GUI). The microfluidic cartridge can automatically handle the complexity of sample preparation, purification, and real-time reverse-transcription Loop-mediated Isothermal Amplification (RT-LAMP). The automation is facilitated by a novel programmable electromagnetic (EM) pulse method. The highly portable analyzer is USB interfaced and integrates cooperating subsystems (electronic, optical and mechanical) into an ultra-compact form factor. Since USB ports are universally available and provide connections for both the power and the data, we anticipate the HIV NAT-on-USB would significantly enhance the device usability by the lay individuals. Through these innovations, we anticipate that HIV self-

testing could be performed as simply as a home blood glucose test. The rapid, low-cost, easy-to-use HIV NAT-on-USB would be particularly useful for the high-risk populations seeking private, highly sensitive self-testing at home.

2 Methods

2.1 Materials and Chemicals

All the electronic and optical components used to build the NAT device (listed in **Supplementary Table S1**) were purchased from Digikey, unless otherwise stated. All RT-LAMP and RT-PCR primers were synthesized by IDT. Isothermal buffer, $MgSO_4$, deoxyribonucleotide triphosphates (dNTPs), Bst 2.0 DNA polymerase, WarmStart reverse transcriptase are from NEB (New England Biolabs). Betaine, Calcein, $MnCl_2$, and EDTA-buffer solution (pH 8.0) were purchased from Sigma-Aldrich. The TaqMan Fast Virus 1-Step Master Mix and the ChargeSwitch™ Total RNA Cell Kit (CS14010) for extracting RNA were purchased from ThermoFisher. The assay was validated in a benchtop real-time PCR instrument (Bio-Rad CFX96). Purified HIV-1 RNAs (Subtype B, USA) were obtained commercially from SeraCare Life Science (cat. 0400-0078). We obtained samples of whole blood collected in potassium EDTA tubes from Innovative Research, Inc (Novi, MI).

2.2 NAT-on-USB analyzer and cartridge instrumentation

The overall design of the instrument is completed by PTC Creo software, and the device housing is fabricated by 3D printing (METHOD X, MakerBot). The PCB is designed in Autodesk Eagle software and fabricated by OSH Park. The electronic components and MCU on the PCB are manually soldered in the laboratory. A resistive-heating element (PWR263S-20-2R00J, Digi-Key) was attached to the backside of the customized aluminum heating plate using thermal paste (AATA-5G, Artic Alumina). A thermistor (95C0606, Digi-Key) was embedded in the center of the heating plate for real-time temperature monitoring. Negative thermal feedback control was performed using N-channel power MOSFET (63J7707, Digi-Key) to maintain the desired temperature during NAT. The one-time use cartridge was designed by AutoCAD, and each layer was patterned using a CO_2 laser cutting machine (Universal Laser Systems). All patterned layers

were aligned and laminated with adhesive solvent. The control GUI software is written in Python, and the GUI establishes connection and communication with the device through USB serial communication.

2.3 HIV-1 RT-LAMP reaction

The RT-LAMP reaction mix (total volume: 25 μL) contains isothermal buffer (20 mM Tris-HCl, 10 mM $(NH_4)_2SO_4$, 50 mM KCl, 2 mM $MgSO_4$, 0.1% Tween 20, pH 8.8), PCR grade H_2O, Betaine (0.8 M), $MgSO_4$ (7 mM), deoxyribonucleotide triphosphates (dNTPs, 1.4 mM), Bst 2.0 DNA polymerase (16U), DNA template, WarmStart reverse transcriptase (2U) and primer sets (0.2 μM F3 and B3c, 1.6 μM FIP and BIP, 0.8 μM LPF and LPB).

2.4 HIV-1 RT-PCR reaction

We used a one-step, two-enzyme RT-PCR protocol for HIV-1 assays. The reaction has a total volume of 20 μL, consisting of 5 μL TaqMan Fast Virus 1-Step Master Mix (cat. 4444432, Thermofisher), forward primer (0.6 μM), reverse primer (0.6 μM), probe (0.25 μM), and 1 μL RNA templates as well as 11 μL PCR grade water. We used a previously validated HIV-1 RT-PCR primer set. (Palmer et al. 2003) The RT-PCR was performed by the following thermal cycling sequences: 50 ℃ for the first five minutes without repeating to reverse transcription reactions which convert HIV-1 RNA into cDNA, then 95℃ for 20 seconds without repeating to initiate amplification, followed by 40 cycles of amplification stage consisting of 3 seconds of 95℃ and 30 seconds of 60℃ thermal-cycling. Primers Forward (5'-CATGTTTTCAGCATTATCAGAAGGA-3') and Reverse (5'-TGCTTGATGTCCCCCCACT-3') (600 nM) and Probe (5′FAM-CCACCCCACAAGATTTAAACACCATGCTAA-Q 3') (250 nM), where FAM indicates a reporter 6-carboxyfluorescein group and Q indicates a 6-carboxytetramethylrhodamine group quencher conjugated through a linker arm nucleotide.

2.5 Mock whole blood HIV sample

Purified HIV-1 RNAs (Subtype B, USA) were obtained commercially from SeraCare Life Science (cat. 0400-0078). As-received RNAs were serially diluted to form linearity panels with concentrations ranging from 1 to 10^5 copies/μL. Aliquots of the linearity panels were stored at -80°C until use. To form the mock whole blood HIV sample, 1 μL of these purified HIV-1 RNAs

was spiked into 99 µL of healthy whole blood to generate 100 µL of mock samples at concentrations from 10 to 10^6 copies/mL immediately before testing. Note that our protocol did not use Proteinase K to inactivate RNases in the whole blood for simplified sample preparation. The volume of the mock sample used in our study is 100 µL unless otherwise indicated.

2.6 Statistical analysis

The fluorescence signals from assays run on the USB device were expressed as the mean of ≥3 independent reactions ± standard deviation (SD). Customized MATLAB code was used to calculate one-way analysis of variance (ANOVA), obtain the optimized threshold for positive/negatives, and calculate linear regression of standard curve.

3 Results and Discussion

3.1 Overall instrumentation

As shown in **Figure 1a**, the HIV NAT-on-USB device consists of a highly portable palm-sized analyzer (footprint of 10×5×5 cm^3, weighing 170 g) and a ready-to-use, disposable reagent cartridge. The inset of **Figure 1a** shows the cartridge design with an overall dimension of 9 cm (l)×1.5 cm (w)×0.58 cm (h). It consists of three-patterned polymethyl methacrylate (PMMA) layers, laminated with an adhesive solvent. The assembled cartridge has a binding chamber (800 µL), a washing chamber (450 µL), and a reaction chamber (25 µL). Each of these functional chambers was separated by an oil valve chamber (Choi et al. 2016). Reagents were preloaded to the cartridge before use.

Figure 1b&c shows the exposed view and the assembled view of the analyzer, respectively. The USB-interfaced analyzer integrates the optical modules (excitation/detection), thermal modules (actuation/sensing), and mechanical modules (PCB coil electromagnet driver). These modules are controlled by a microcontroller unit (MCU) to fully automate the sample-to-answer process on the disposable cartridge. The working principle of the optical and thermal modules is similar to those used in our previous AnyMDx instrument (Choi et al. 2016), with modifications in spatial configurations. After assembly, we validated that the optical sensor has a linear response to the Calcein concentration from 0 to 25 µM (**Supplementary Figure S1**), confirming its

suitability for real-time monitoring of the amplification process. In addition, we validated that the resistive heating module can reach the desired 60°C within 1.5 mins and the root mean squared (RMS) value of the temperature is 0.53°C after stabilization (**Supplementary Figure S2**), which can meet the temperature requirement of the LAMP assay (Rudolph et al. 2015). For actuating the nucleic acid-bearing magnetic beads on the cartridge, we designed a double-sided planar coil array on a printed circuit board (PCB). This PCB coil can be programmed to generate a localized electromagnetic (EM) field for actuating a permanent magnet (**Figure 1d**).

Figure 1e shows the overall workflow of the HIV NAT-on-USB. The user would self-collect ~100 μL of finger-prick blood using an exact volume transfer pipet and drop it into a collecting tube pre-filled with 800 μL lysis buffer, 200 μL binding buffer, and 15 μL charge switchable magnetic beads. After the blood is collected into the lysis tube, the user can shake the tube to promote the mixing and binding. After 1 min, the lysate is loaded onto the cartridge through the extruded inlet, which can be completely sealed with a screw cap by hand tightening. The sealed cartridge is then inserted along a sliding rail into the analyzer through a hinged intake lid. After closing the lid, the analyzer is connected to a personal computer (PC) through a USB port. A customized PC graphical user interface (GUI) was developed for interfacing the analyzer and interpreting the data in a user-friendly way. The GUI can automatically detect a new analyzer connection, request user information, initiate the nucleic acid test, and report the 'yes/no' qualitative result (see **Supplementary Figure S3** for software flowchart). It is noteworthy that the USB-interfaced analyzers can be used in a plug-and-play (PnP) fashion. In addition, multiple USB-interfaced analyzers can be simultaneously and independently connected to a PC through a USB hub for enhanced throughput, if needed. The material cost per test is $3.30 per reagent cartridge and $69.43 per analyzer (**Supplementary Table S1 & Table S2**). It is noteworthy that the microfluidic cartridge is an enclosed system after the sample is loaded. It is disposable after each test. Therefore, cross-contamination between tests is not a concern. The overall HIV NAT-on-USB workflow requires minimal user intervention and is simple enough for the laypersons to perform HIV self-testing. **Supplementary Video S1** shows the overall workflow of the test.

3.2 Programmable electromagnetic pulse for sample preparation on cartridge

We have previously demonstrated the use of charge-switchable magnetic beads for streamlining nucleic acid binding, purification, and elution by rotating a microfluidic disc against

a stationary magnet (Choi et al. 2016). To completely remove the bulky moving parts for actuating the magnetic beads in the NAT-on-USB device, we here further developed a programmable electromagnetic method using double-sided planar coil arrays (**Figure 2a**). The planar coil is designed into two layers in a single PCB. There are 12 coils on the top layer and 11 coils on the bottom layer (1×23 array). The permanent magnet can be programmed to the center of any of these 23 coils. This is because a deviation from the 'ON' coil will result in a restoring force to bring the permanent magnet to its equilibrium position (center of the 'ON' coil) (**Figure 2b-d**).

It is noteworthy that several previous studies (Beyzavi and Nguyen 2009; Chiou et al. 2013; Rida et al. 2003) had tried to use planar coils to generate electromagnets for direct manipulation of the magnetic beads. However, due to the small size and weak relative magnetic susceptibility of magnetic beads (χ_r<<1), the magnetic beads must be significantly polarized by strong permanent magnets. Moreover, a strong electromagnet field with ~ 1 A DC current is required, in which excessive heat can be generated due to the Joule heating (Chiou et al. 2013). Our approach here uses the programmable pulsed EM field to actuate a permanent magnet that further controls the magnetic beads on the cartridge (**Figure 2e&f**). Since the permanent magnet itself has a substantial susceptibility, a small electromagnet field (*i.e.*, a reduced power consumption) is sufficient to drive its motion. In addition, the actuation of the permanent magnet only requires 100 ms of 'ON' time on the desired coil. With this pulsed operation, we found that a minimum of 450 mA is sufficient to actuate the permanent magnet in our device. The temperature generated by the Joule heating was found to be operation frequency-dependent. At the normal 1 Hz operation, the measured max temperature did not exceed 30 °C for 5 min operation (**Figure 2g&h**), suggesting that the reagents and assays in the cartridge would not be affected by the electromagnetic actuation, alleviating the overheating problems in previous methods (Chiou et al. 2013).

Figure 3 illustrates the automated sample preparation and amplification on cartridges enabled by the EM actuation of charge-switchable magnetic beads (Choi et al. 2016). In the first step, the negatively charged RNAs in the lysate bind to the positively charged magnetic beads at pH 5 in the binding chamber. During the binding process, the permanent magnetic under the cartridge was actuated back and forth at a frequency of 1/3 Hz to ensure thorough mixing. In the second step, the RNA binding beads were transferred to the washing chamber (buffered at pH 7) by the EM array. The beads were horizontally agitated by the programmed EM sequence at 1/3 Hz. In the third step, the washed beads were transferred to the reaction chamber with the master mix buffered

at pH 8.8. The RNAs were directly eluted to the master mix due to the positive charge on the magnetic bead surface. After elution, these magnetic beads were moved away from the reaction chamber (step 4) before starting the RT-LAMP reaction (step 5). The entire sample preparation could be completed in less than 15 minutes with minimum user interaction. **Supplementary Video S2** presents a typical workflow of the EM array-enabled automated sample preparation and amplification on the cartridge.

3.3 Copy Number sensitivity of HIV-1 RT-LAMP

We used a previously validated HIV-1 LAMP primer set against the highly conserved region of the integrase gene within subtype B (Curtis et al. 2012) with a modified fluorescent reporter of Calcein (Tomita et al. 2008). We first validated the intrinsic copy number sensitivity of the HIV-1 RT-LAMP assay by performing the RT-LAMP reaction against the quantitative panel of HIV-1 RNAs at concentrations ranging from 10^5 copies/μL down to 1 copy/μL. **Figure 4** summarized the RT-LAMP primers, the reaction setup, and the real-time RT-LAMP results. As shown in **Figure 4c-f,** the copy number sensitivity of the HIV-1 RT-LAMP was determined to be four copies. Changes in temperature or storage time can affect the performance of LMAP. The prepared LAMP should be kept in a refrigerated environment, and it is best to use it immediately.

3.4 Whole blood HIV-1 RT-LAMP assay

To further test the impact of the whole blood matrix and the reagent on the HIV-1 RT-LAMP assay, we formed mock HIV-1 positive samples by spiking the HIV-1 RNA into healthy whole blood. The 100 μL of mock samples at concentrations from 10 to 10^6 copies/mL were mixed with 500 μL lysis buffer, 200 μL binding buffer, and 15 μL charge switchable magnetic beads for lysis and binding. The beads were then washed with 450 μL of washing buffer. The RNAs were directly eluted into a 25 μL master mix for RT-LAMP reaction. **Figure 5a** presents the real-time RT-LAMP results (each concentration was repeated six times). **Figure 5b** shows the fluorescent image of the reaction tubes under the ultraviolet (UV) light. **Figure 5c** shows the gel electrophoresis results in 2% agarose gel, in which clear ladder-like patterns with multiple bands of different molecular sizes were observed due to the stem-loop DNA structures with several inverted repeats within LAMP amplicons (Notomi et al. 2000; Tomita et al. 2008). The fluorescent image and the gel images agreed well with each other.

To estimate the LoD of whole blood HIV-1 RT-LAMP assay, we examined the hit rates at different RNA concentrations (Holstein et al. 2015). The hit rate is defined as the number of amplified samples over all samples. As shown in **Figure 5d,** the LoD of the whole blood RT-LAMP assay is determined to be 214 copies/mL at the 95% confidence level. This LoD is higher than that obtained with the HIV-1 quantitative panels (4 copies, **Figure 4e**). We believe the following factors are responsible for the deteriorated LoD in the whole blood samples. First, although we used the spiked sample as soon as we prepared it, the HIV-1 RNA can still experience a certain degree of degradation in the whole blood. Second, inhibitors could exist with the whole blood sample. Third, there is a possibility of material loss during the sample preparation process. We further examined the time to positive as a function of the RNA concentrations in whole blood. As shown in **Figure 5e,** linear fit produced the R^2 with 0.89, similar to those obtained with the HIV-1 quantitative panels (**Figure 4d**).

3.5 Intra- and inter-device performance test

After validating the automated sample preparation and the HIV-1 RT-LAMP assay, we went out to test the intra- and inter-device performances. It is noteworthy that the multiple USB-interfaced analyzers can be used simultaneously and independently in a plug-and-play (PnP) fashion (**Figure 6a** and **Supplementary Video S1)**.

For the intra-device verification, we tested a series of mock samples with different HIV-1 RNA concentrations. **Figure 6b** shows the real-time data obtained from testing a triplicate panel of these samples with a single USB interfaced analyzer. As shown, HIV-1 RNA concentrations at 500 copies per mL of whole blood were all amplified successfully (in par with these obtained in the tube, **Figure 5d**). **Figure 6c** shows the time to positive as a function of the input RNA concentrations. A linear fit produced the R^2 with 0.85, indicating the feasibility of using the USB-interfaced analyzer for a semi-quantitative test on the whole blood (*i.e.*, differentiating between high, medium, and low viral load).

For the inter-device verification, we tested four independent devices with multiple triplicated mock samples. **Supplementary Figure S4** summarizes the real-time data obtained from these tests. We benchmarked the time to positive between any two devices and examined their Pearson correlation coefficient. As shown in **Figure 6d**, the device to device showed Pearson correlation coefficients ranging from 0.79 to 0.92, suggesting a good quantitative

agreement between these devices.

To determine the diagnostic ability of the HIV NAT-on-USB, we tested a total of 104 whole blood samples (52 negatives and 52 positives) with four different analyzers. The 52 positive samples were constructed by spiking the HIV-1 RNA into 100 μL human whole blood to form a concentration of 1000 copies/mL, a clinically relevant viral load threshold used for routine monitoring of HIV in resource-limited settings (Ellman et al. 2017; Manoto et al. 2018). We examined the fluorescence values for all samples at 60 min (**Figure 6e)**. As shown, the RFU values of positives were significantly higher than that of the healthy controls. To find the optimal fluorescence threshold to differentiate the positives and negatives, we analyzed the receiver operating characteristic (ROC) curve (Bewick et al. 2004; Zweig and Campbell 1993) by varying the threshold from 1 to 500 RFU. In general, increasing the threshold will improve the specificity but deteriorate the sensitivity. The optimal RFU threshold from ROC analysis is 43 (dashed line in **Figure 6e**). The inset of Figure 6e summarized the diagnostic performance with this optimized threshold. 50 out of 52 positives were detected as true positives, and 46 out of 52 negatives were detected as true negatives. The sensitivity, and specificity of the test was 96.2% (95% CI=90.9%-100%) and 88.5% (95% CI= 79.8%-97.1%). The tests performed with all four different devices showed excellent accuracy (93%) in differentiating the clinically relevant viral load threshold at 1000 copies/mL.

4 Conclusions

In summary, we developed an integrated 'finger-prick blood sample in, answer out' full auto sample preparation and detection HIV NAT device towards HIV self-testing using 100 μL of a self-obtained finger-prick blood sample. The device consists of an ultra-compact NAT-on-USB analyzer and a ready-to-use microfluidic cartridge. The test requires simple steps from the user to drop the finger-prick blood sample into a collection tube with lysis buffer and load the lysate onto the microfluidic cartridge, and the testing result can be easily interpreted by the user through a GUI. We fully automated the process of on-chip RNA extraction, purification, and isothermal amplification from a whole blood sample and achieved an LoD of 214 copies per mL of whole blood at the 95% confidence level. Although the HIV NAT-on-USB device is designed for self-testing, the test can be easily scaled up to conduct multiple tests simultaneously through a USB

hub. This makes the device also suitable for use in primary care settings as well. To further develop this technology for self-testing, there are several outstanding issues we need to address, including validation with clinical HIV-positive samples, evaluating performance across different subtypes of HIV-1, incorporating an internal control, and the lyophilization of the LAMP reagents to allow ambient storage at room temperature. With these efforts, we anticipate the rapid, low-cost, easy-to-use HIV NAT-on-USB device could enable laypersons to perform highly sensitive self-testing at home.

Author contributions

T.L., G.C., and A.K. performed the instrument and integration. T.L. and Z.T. developed and validated the RT-LAMP and RT-PCR assay. T.L. and A.J.P. developed the sample preparation protocol. T.L. performed the validation of the device. W. Guan conceived the concept and supervised the study. All authors analyzed the data and co-wrote the manuscript.

Conflicts of interest

A provisional patent related to the technology described herein is filed.

Acknowledgments

This work was supported by the National Institutes of Health (R61AI147419), and National Science Foundation (1912410 & 1902503). Any opinions, findings, and conclusions or recommendations expressed in this work are those of the authors and do not necessarily reflect the views of the National Science Foundation and National Institutes of Health.

Figures and Captions

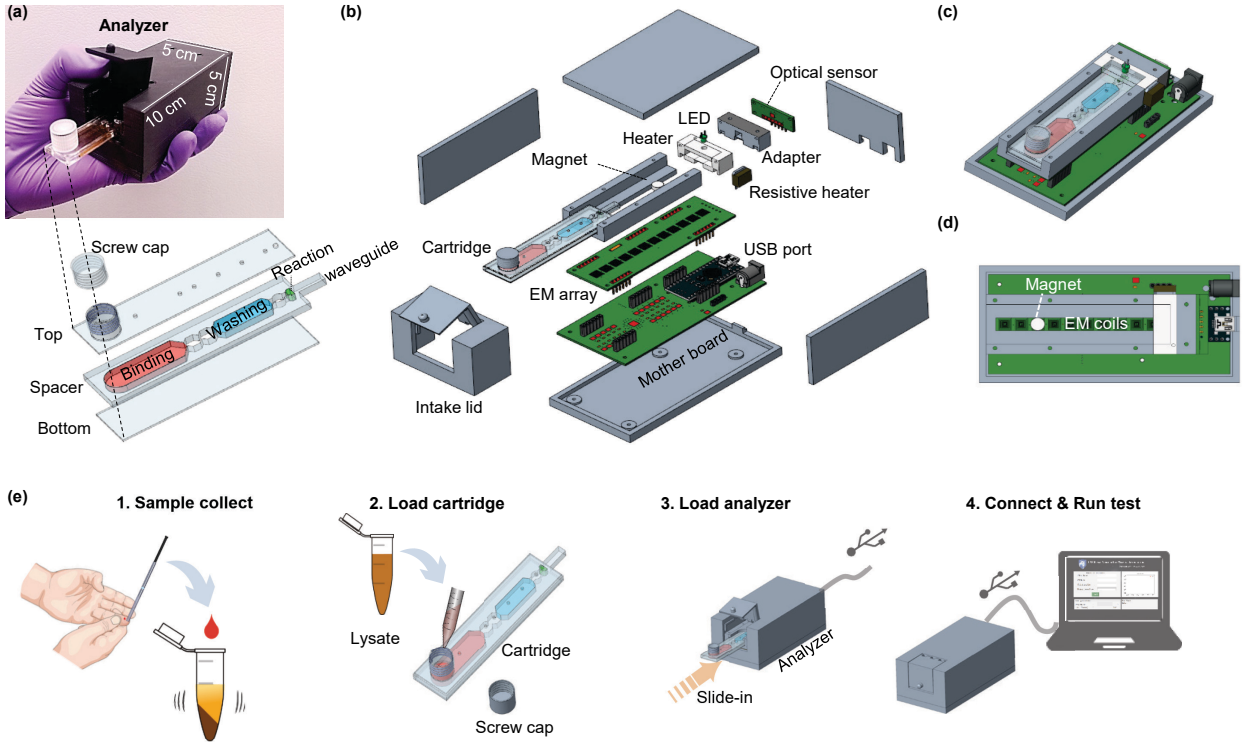

Figure 1 Overall HIV NAT-on-USB device and microfluidic cartridge design. (a) Photo image of the device held by hand. The enlarged inset shows the exposed view of the cartridge. (b) Exposed view of the analyzer. The analyzer was designed to be USB-interfaced for data connection. Optical, thermal, and electromagnetic array subsystems are seamlessly integrated to perform streamlined nucleic acid testing. (c) The assembled view of the analyzer with the cartridge in the operation position. (d) Top view of the analyzer, showing the electromagnetic array and the permanent magnet. (e) Overall operation workflow of HIV NAT-on-USB device. The user self-collects 100 μL of finger-prick blood into the lysis tube (premixed with lysis buffer and the magnetic beads) and shakes it for thorough mixing (step 1). The lysate mixture is loaded to the binding chamber of the microfluidic cartridge. After loading, the cartridge inlet is sealed with a screw cap (step 2). The sealed cartridge is then inserted into the USB analyzer (step 3). The analyzer is connected to a PC through the USB port. The test will be automatically recognized and administrated by a graphic user interface (GUI). The final positive/negative results will be displayed at the end of the automated process (step 4).

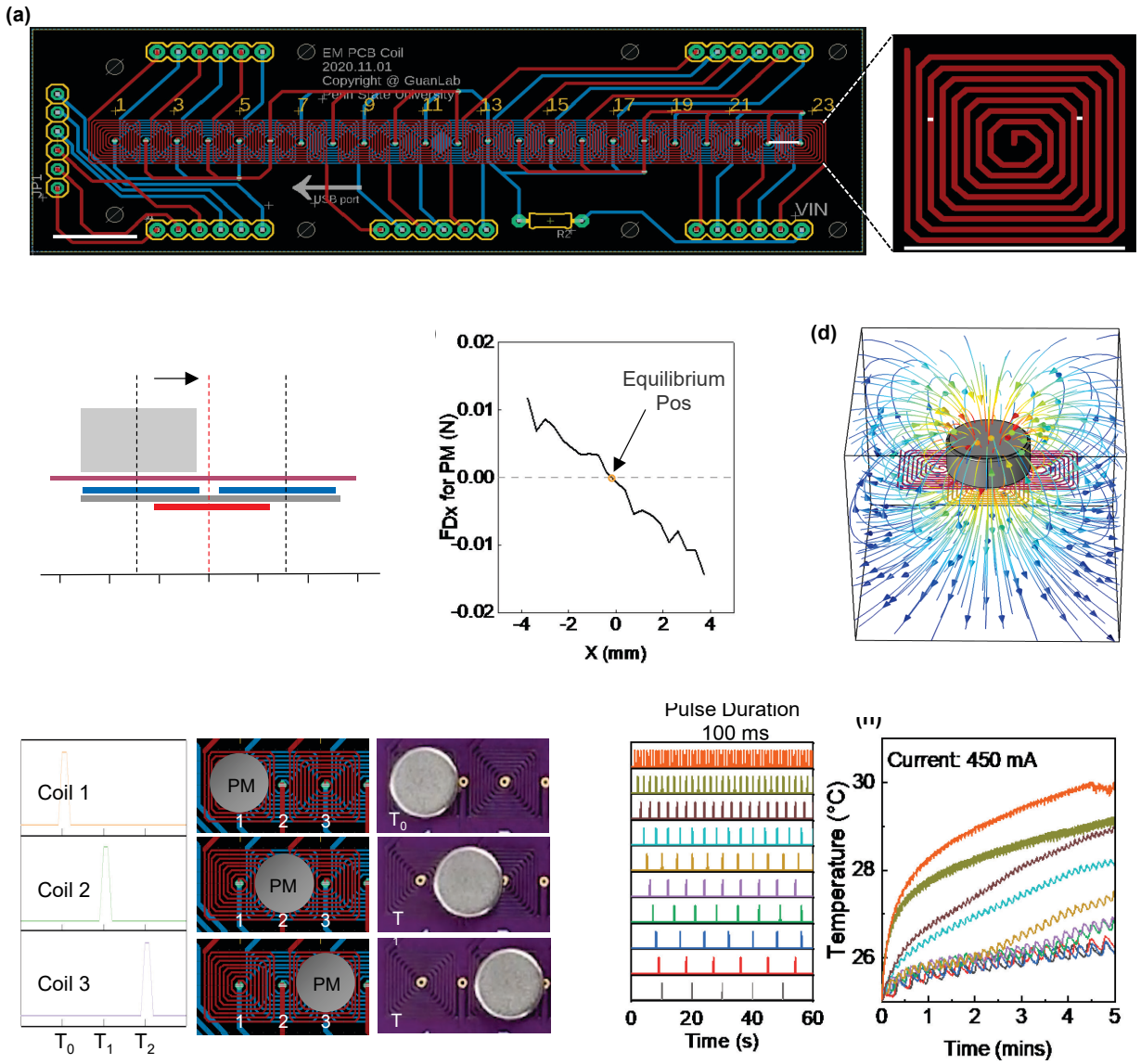

Figure 2 (a) The PCB design of the double-sided planar coil array. The planar coil is designed as two layers in a single PCB with a vertical distance of 0.78 mm. Each rectangular coil has a winding width of 170 µm, a spiral pitch of 170 µm, a thickness of 35 µm, and nine turns (enlarged inset). The coils on the top and bottom layers are offset by 3.6 mm horizontally, yielding an effective motion step of 3.6 mm. (b) The operation diagram of the permanent magnet being moved from an initial position to a new adjacent position by turning on a specific coil (coil 2 in this case). (c) Calculated force on the permanent magnet as a function of the relative displacement of the permanent magnet to the coil center. (d) COMSOL simulation of the electromagnetic field generated by the planar coil. (e) The sequence of the current pulse to move the permanent magnet from position 1 to position 3. Each pulse is 100 ms in duration. (f) The corresponding permanent magnet position at each time spot during the pulsed operation. (g) Joule heating evaluation for the programmable electromagnetic pulse. The current pulse waveform with 0.1 Hz to 1 Hz operating frequencies. The duration of each pulse is fixed at 100 ms. (h) The time course of the temperature

measured on the planar coil surface at different operating frequencies (color corresponding to these in (g)). The current pulse amplitude is 450 mA. With 0.1 to 1 Hz operation frequencies, the measured temperature does not exceed 30 °C for 5 min of operation.

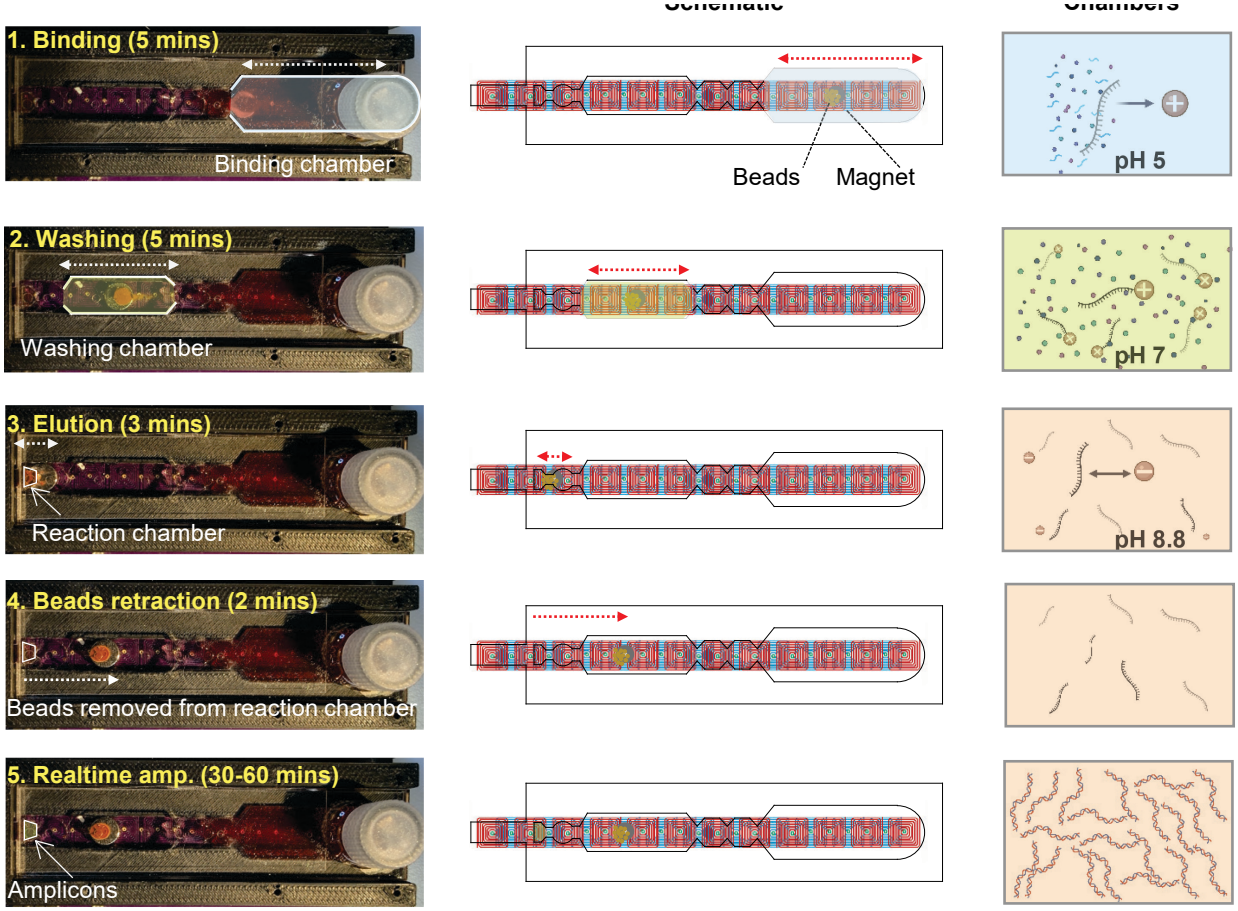

Figure 3 Automated sample preparation and amplification on cartridges enabled by the EM pulsed actuation of charge-switchable magnetic beads. The entire sample preparation could be completed in less than 15 minutes with minimum user interaction. The left, middle and right panels show the photo image of the actual device, the schematic of the relative position of the cartridge chambers to the EM driven magnet, and the schematic interactions of molecules with magnetic beads, respectively. In step 1, the negatively charged RNAs in the lysate binds to the positively charged magnetic beads at pH 5 in the binding chamber. In step 2, RNA binding beads were transferred to the washing chamber (buffered at pH 7). In step 3, the washed beads were transferred to the reaction chamber with the master mix buffered at pH 8.8. After elution, these magnetic beads were moved away from the reaction chamber (step 4) before starting the RT-LAMP reaction (step 5).

Primer	Sequence (5' → 3')
F3	AGTTCCCTTAGATAAAGACTT
B3	CCTACATACAAATCATCCATGT
FIP	GTGGAAGCACATTGTACTGATATCTTTTTGGAAGTATACTGCATTTACCAT
BIP	GGAAAGGATCACCAGCAATATTCCTCTGGATTTTGTTTTCTAAAAGGC
Loop F	GGTGTCTCATTGTTTATACTA
Loop B	GCATGACAAAAATCTTAGA

(b)

Component	Volume (µl)/test	Final Concentration
Isothermal Buffer	2.5	1 X
F3	0.25	0.2 µM
B3	0.25	0.2 µM
FIP	2	1.6 µM
BIP	2	1.6 µM
LF	1	0.8 µM
LB	1	0.8 µM
Betaine	4	0.8 M
MgSO4	1.75	7 mM
Calcein	0.63	25 µM
MnCl2	1.88	75 µM
dNTP Mix	3.5	1.4 mM
Bst polymerase	2	0.64 U/ul
Warmstart RT	0.5	0.3 U/ul
RNA sample	1	1 ul/rxn
PCR Grade Water	0.75	-

(c)

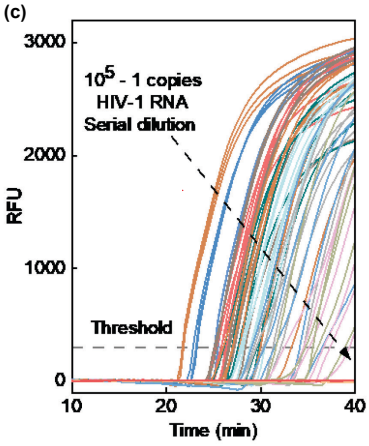

(d)

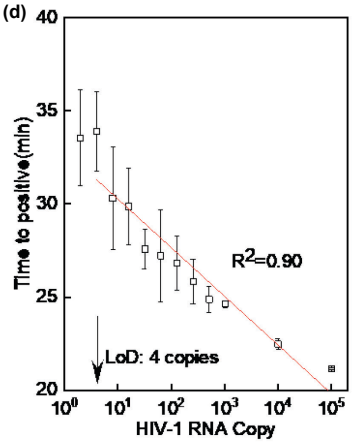

(e)

HIV-1 RNA (copy)	1	2	4	8	16	32	64	128	256	512	1024	10^4	10^5
No. positive/ no. of replicates	0/6	4/6	6/6	6/6	6/6	6/6	6/6	6/6	6/6	6/6	6/6	6/6	6/6
Hit rate (%)	0%	66.7%	100%	100%	100%	100%	100%	100%	100%	100%	100%	100%	100%

Figure 4 Validation of the HIV-1 RT-LAMP assay with the quantitative panel. (a) Primer set for HIV-1 subtype B RT-LAMP amplification. (b) RT-LAMP reaction setup. (c) Real-time RT-LAMP amplification data with serially diluted HIV RNA standards (each concentration was repeated six times). (d) Time to positive value at different HIV-1 RNA concentrations. The time to positive is defined as the time needed for the RFU to reach the threshold level of 300 (dashed line in c). (e) Summary of the hit rate. All six reactions with four or more copies of RNAs can be amplified successfully. The copy number sensitivity of the HIV-1 RT-LAMP was determined to be four copies.

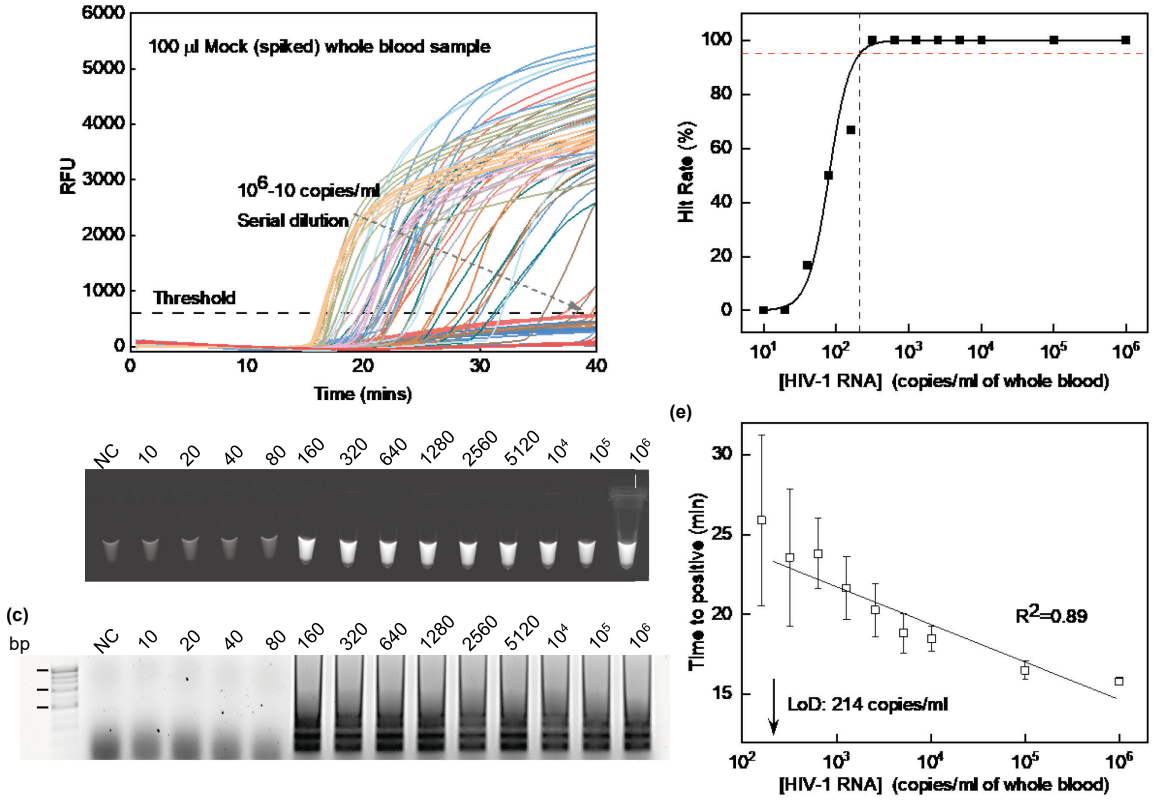

Figure 5 RT-LAMP assay validation with spiked whole blood mock sample. (a) RT-LAMP amplification curves with serially diluted HIV RNA standards. (b) Photo image of RT-LAMP products observed in the reaction tubes under a UV light. (c) Gel image of RT-LAMP products analyzed by agarose gel electrophoresis. (d) The extracted hit rate at various RNA concentrations to establish the assay LoD, which is determined to be 214 copies/mL at the 95% confidence level. (e) Time to positive value at different HIV-1 RNA concentrations in whole blood.

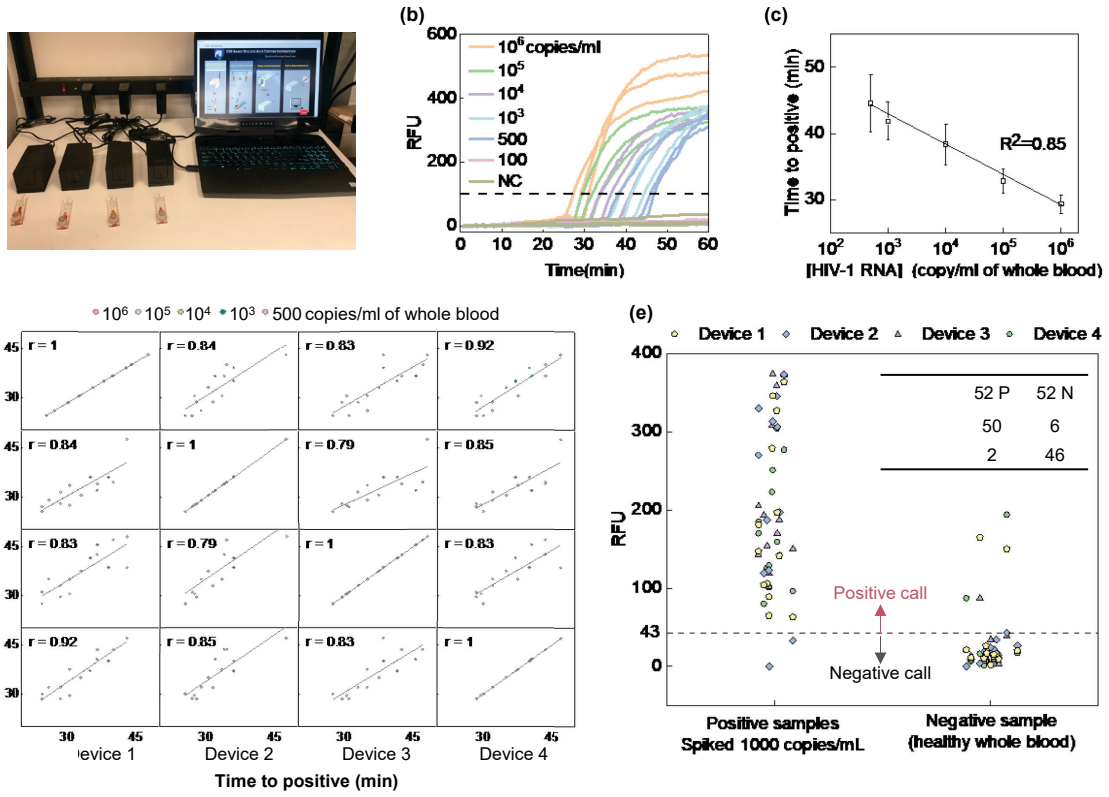

Figure 6 Intra- and inter-device performance. (a) Photo image showing multiple analyzers being used simultaneously through a single USB hub. (b) The real-time RT-LAMP data in the intra-device test with a serially diluted mock blood sample. Each concentration was tested in triplicates. (c) Extracted time to positive value for the intra-device test. (d) The scattering plot of the time to positive value between two devices. (e) The end-point fluorescence values for a total of 104 whole blood samples (52 negatives and 52 positives) were tested with four different analyzers. The dashed line of the value 43 is the receiver operating characteristics (ROC)-optimized fluorescence threshold. The inset table shows the summarization of the results.

References

Bertagnolio, S., Parkin, N.T., Jordan, M., Brooke, J., Garcia-Lerma, J.G., 2010. Dried blood spots for HIV-1 Drug Resistance and Viral Load Testing: A Review of Current Knowledge and WHO Efforts for Global HIV Drug Resistance Surveillance. Aids Reviews 12(4), 195-208.

Bewick, V., Cheek, L., Ball, J., 2004. Statistics review 13: receiver operating characteristic curves. Critical care 8(6), 1-5.

Beyzavi, A., Nguyen, N.T., 2009. One-dimensional actuation of a ferrofluid droplet by planar microcoils. J Phys D Appl Phys 42(1).

Chiou, C.-H., Shin, D.J., Zhang, Y., Wang, T.-H., 2013. Topography-assisted electromagnetic platform for blood-to-PCR in a droplet. Biosensors and Bioelectronics 50, 91-99.

Choi, G., Prince, T., Miao, J., Cui, L.W., Guan, W.H., 2018. Sample-to-answer palm-sized nucleic acid testing device towards low-cost malaria mass screening. Biosensors & bioelectronics 115, 83-90.

Choi, G., Song, D., Shrestha, S., Miao, J., Cui, L.W., Guan, W.H., 2016. A field-deployable mobile molecular diagnostic system for malaria at the point of need. Lab Chip 16(22), 4341-4349.

Curtis, K.A., Niedzwiedz, P.L., Youngpairoj, A.S., Rudolph, D.L., Owen, S.M., 2014. Real-Time Detection of HIV-2 by Reverse Transcription-Loop-Mediated Isothermal Amplification. J Clin Microbiol 52(7), 2674-2676.

Curtis, K.A., Rudolph, D.L., Morrison, D., Guelig, D., Diesburg, S., McAdams, D., Burton, R.A., LaBarre, P., Owen, M., 2016. Single-use, electricity-free amplification device for detection of HIV-1. Journal of virological methods 237, 132-137.

Curtis, K.A., Rudolph, D.L., Nejad, I., Singleton, J., Beddoe, A., Weigl, B., LaBarre, P., Owen, S.M., 2012. Isothermal amplification using a chemical heating device for point-of-care detection of HIV-1. PloS one 7(2), e31432.

Curtis, K.A., Rudolph, D.L., Owen, S.M., 2008. Rapid detection of HIV-1 by reverse-transcription, loop-mediated isothermal amplification (RT-LAMP). Journal of virological methods 151(2), 264-270.

Curtis, K.A., Rudolph, D.L., Owen, S.M., 2009. Sequence-specific detection method for reverse transcription, loop-mediated isothermal amplification of HIV-1. J Med Virol 81(6), 966-972.

Damhorst, G.L., Duarte-Guevara, C., Chen, W., Ghonge, T., Cunningham, B.T., Bashir, R., 2015. Smartphone-Imaged HIV-1 Reverse-Transcription Loop-Mediated Isothermal Amplification (RT-LAMP) on a Chip from Whole Blood. Engineering 1(3), 324-335.

de la Fuente, L., Rosales-Statkus, M.E., Hoyos, J., Pulido, J., Santos, S., Bravo, M.J., Barrio, G., Fernandez-Balbuena, S., Belza, M.J., Madrid Rapid, H.I.V.T.G., 2012. Are participants in a street-based HIV testing program able to perform their own rapid test and interpret the results? PloS one 7(10), e46555.

Dineva, M.A., Mahilum-Tapay, L., Lee, H., 2007. Sample preparation: a challenge in the development of point-of-care nucleic acid-based assays for resource-limited settings. The Analyst 132(12), 1193-1199.

Ellman, T.M., Alemayehu, B., Abrams, E.J., Arpadi, S., Howard, A.A., El‐Sadr, W.M., 2017. Selecting a viral load threshold for routine monitoring in resource‐limited settings: optimizing individual health and population impact. Journal of the International AIDS Society 20(Suppl 7).

Fidler, S., Lewis, H., Meyerowitz, J., Kuldanek, K., Thornhill, J., Muir, D., Bonnissent, A., Timson, G., Frater, J., 2017. A pilot evaluation of whole blood finger-prick sampling for point-of-care HIV viral load measurement: the UNICORN study. Scientific reports 7(1), 13658.

Frith, L., 2007. HIV self-testing: a time to revise current policy. Lancet 369(9557), 243-245.
Frye, V., Koblin, B.A., 2017. HIV self-testing in high-risk populations. The lancet. HIV 4(6), e232-e233.
Fund, T.G., 2022. List of HIV Diagnostic test kits and equipments classified according to the Global Fund Quality Assurance Policy https://www.theglobalfund.org/media/5878/psm_productshiv-who_list_en.pdf.
Guichet, E., Serrano, L., Laurent, C., Eymard-Duvernay, S., Kuaban, C., Vidal, L., Delaporte, E., Ngole, E.M., Ayouba, A., Peeters, M., 2018. Comparison of different nucleic acid preparation methods to improve specific HIV-1 RNA isolation for viral load testing on dried blood spots. Journal of virological methods 251, 75-79.
Holstein, C.A., Griffin, M., Hong, J., Sampson, P.D., 2015. Statistical method for determining and comparing limits of detection of bioassays. Analytical chemistry 87(19), 9795-9801.
Iwuji, C., Newell, M.L., 2017. HIV testing: the 'front door' to the UNAIDS 90-90-90 target. Public health action 7(2), 79.
Johnson, C.C., Corbett, E.L., 2016. HIV self-testing to scale up couples and partner testing. The lancet. HIV 3(6), e243-244.
LabCorp, HIV Specimen Collection Guide. https://monogrambio.labcorp.com/sites/default/files/2019-11/L12159-0516-5.pdf.
Liao, S.C., Peng, J., Mauk, M.G., Awasthi, S., Song, J., Friedman, H., Bau, H.H., Liu, C., 2016. Smart Cup: A Minimally-Instrumented, Smartphone-Based Point-of-Care Molecular Diagnostic Device. Sens Actuators B Chem 229, 232-238.
Liu, C., Geva, E., Mauk, M., Qiu, X., Abrams, W.R., Malamud, D., Curtis, K., Owen, S.M., Bau, H.H., 2011. An isothermal amplification reactor with an integrated isolation membrane for point-of-care detection of infectious diseases. Analyst 136(10), 2069-2076.
Manoto, S.L., Lugongolo, M., Govender, U., Mthunzi-Kufa, P., 2018. Point of care diagnostics for HIV in resource limited settings: an overview. medicina 54(1), 3.
Mauk, M., Song, J., Bau, H.H., Gross, R., Bushman, F.D., Collman, R.G., Liu, C., 2017. Miniaturized devices for point of care molecular detection of HIV. Lab Chip 17(3), 382-394.
Mazzola, L., Pérez-Casas, C., 2015. HIV/AIDS diagnostics technology landscape 5th edition. UNITAID, 66-68.
Mugo, P.M., Micheni, M., Shangala, J., Hussein, M.H., Graham, S.M., Rinke de Wit, T.F., Sanders, E.J., 2017. Uptake and Acceptability of Oral HIV Self-Testing among Community Pharmacy Clients in Kenya: A Feasibility Study. PloS one 12(1), e0170868.
Myers, F.B., Henrikson, R.H., Bone, J.M., Lee, L.P., 2013. A handheld point-of-care genomic diagnostic system. PloS one 8(8), e70266.
Ng, O.T., Chow, A.L., Lee, V.J., Chen, M.I., Win, M.K., Tan, H.H., Chua, A., Leo, Y.S., 2012. Accuracy and user-acceptability of HIV self-testing using an oral fluid-based HIV rapid test. PloS one 7(9), e45168.
Ng, O.T., Tan, M.T., 2013. HIV self-testing: money matters. Clin Infect Dis 57(5), 771-772.
Notomi, T., Okayama, H., Masubuchi, H., Yonekawa, T., Watanabe, K., Amino, N., Hase, T., 2000. Loop-mediated isothermal amplification of DNA. Nucleic acids research 28(12), E63.
Ocwieja, K.E., Sherrill-Mix, S., Liu, C., Song, J., Bau, H., Bushman, F.D., 2015. A reverse transcription loop-mediated isothermal amplification assay optimized to detect multiple HIV subtypes. PloS one 10(2), e0117852.
Odari, E.O., Maiyo, A., Lwembe, R., Gurtler, L., Eberle, J., Nitschko, H., 2015. Establishment and evaluation of a loop-mediated isothermal amplification (LAMP) assay for the semi-quantitative

detection of HIV-1 group M virus. Journal of virological methods 212, 30-38.
Palmer, S., Wiegand, A.P., Maldarelli, F., Bazmi, H., Mican, J.M., Polis, M., Dewar, R.L., Planta, A., Liu, S., Metcalf, J.A., 2003. New real-time reverse transcriptase-initiated PCR assay with single-copy sensitivity for human immunodeficiency virus type 1 RNA in plasma. Journal of clinical microbiology 41(10), 4531-4536.
Parekh, B.S., Ou, C.-Y., Fonjungo, P.N., Kalou, M.B., Rottinghaus, E., Puren, A., Alexander, H., Hurlston Cox, M., Nkengasong, J.N., 2018. Diagnosis of human immunodeficiency virus infection. Clinical microbiology reviews 32(1), e00064-00018.
Phillips, E.A., Moehling, T.J., Bhadra, S., Ellington, A.D., Linnes, J.C., 2018. Strand Displacement Probes Combined with Isothermal Nucleic Acid Amplification for Instrument-Free Detection from Complex Samples. Anal Chem 90(11), 6580-6586.
Phillips, E.A., Moehling, T.J., Ejendal, K.F.K., Hoilett, O.S., Byers, K.M., Basing, L.A., Jankowski, L.A., Bennett, J.B., Lin, L.K., Stanciu, L.A., Linnes, J.C., 2019. Microfluidic rapid and autonomous analytical device (microRAAD) to detect HIV from whole blood samples. Lab Chip 19(20), 3375-3386.
Rida, A., Fernandez, V., Gijs, M.A.M., 2003. Long-range transport of magnetic microbeads using simple planar coils placed in a uniform magnetostatic field. Appl Phys Lett 83(12), 2396-2398.
Rudolph, D.L., Sullivan, V., Owen, S.M., Curtis, K.A., 2015. Detection of Acute HIV-1 Infection by RT-LAMP. PloS one 10(5), e0126609.
Safavieh, M., Kanakasabapathy, M.K., Tarlan, F., Ahmed, M.U., Zourob, M., Asghar, W., Shafiee, H., 2016. Emerging Loop-Mediated Isothermal Amplification-Based Microchip and Microdevice Technologies for Nucleic Acid Detection. Acs Biomater-Sci Eng 2(3), 278-294.
Sarkar, A., Mburu, G., Shivkumar, P.V., Sharma, P., Campbell, F., Behera, J., Dargan, R., Mishra, S.K., Mehra, S., 2016. Feasibility of supervised self-testing using an oral fluid-based HIV rapid testing method: a cross-sectional, mixed method study among pregnant women in rural India. Journal of the International AIDS Society 19(1), 20993.
Singleton, J., Osborn, J.L., Lillis, L., Hawkins, K., Guelig, D., Price, W., Johns, R., Ebels, K., Boyle, D., Weigl, B., LaBarre, P., 2014. Electricity-free amplification and detection for molecular point-of-care diagnosis of HIV-1. PloS one 9(11), e113693.
Spielberg, F., Levine, R.O., Weaver, M., 2004. Self-testing for HIV: a new option for HIV prevention? Lancet Infect Dis 4(10), 640-646.
Stone, M., Bainbridge, J., Sanchez, A.M., Keating, S.M., Pappas, A., Rountree, W., Todd, C., Bakkour, S., Manak, M., Peel, S.A., 2018. Comparison of detection limits of fourth-and fifth-generation combination HIV antigen-antibody, p24 antigen, and viral load assays on diverse HIV isolates. Journal of clinical microbiology 56(8), e02045-02017.
Tomita, N., Mori, Y., Kanda, H., Notomi, T., 2008. Loop-mediated isothermal amplification (LAMP) of gene sequences and simple visual detection of products. Nature protocols 3(5), 877.
Wang, X., Seo, D.J., Lee, M.H., Choi, C., 2014. Comparison of conventional PCR, multiplex PCR, and loop-mediated isothermal amplification assays for rapid detection of Arcobacter species. J Clin Microbiol 52(2), 557-563.
WHO, 2021. HIV/AIDS.
Zolopa, A.R., 2010. The evolution of HIV treatment guidelines: current state-of-the-art of ART. Antiviral research 85(1), 241-244.
Zweig, M.H., Campbell, G., 1993. Receiver-operating characteristic (ROC) plots: a fundamental evaluation tool in clinical medicine. Clinical chemistry 39(4), 561-577.